ACS APPLIED MATERIALS & INTERFACES

Research Article

www.acsami.org

Highly Flexible and Tough Concentric Triaxial Polystyrene Fibers

Shaohua Jiang,[†] Gaigai Duan,[†] Eyal Zussman,[‡] Andreas Greiner,[†] and Seema Agarwal*,[†]

[†]Macromolecular Chemistry II and Bayreuth Center for Colloids and Interfaces, Universität Bayreuth, Universitätsstraße 30, 95440 Bayreuth, Germany

[‡]Faculty of Mechanical Engineering, Technion, Israel Institute of Technology, Haifa 32000, Israel

ABSTRACT: A combination of appropriate reinforcing material and morphology led to the highly tough, flexible, and strong polystyrene fibers by electrospinning. Concentric fiber morphology with reinforcing elastomeric thermoplastic polyurethane (TPU) sandwiched between the two layers of polystyrene made by a special nozzle (triaxial) showed toughness of >270 J g^{-1} and 300% elongation without any cracks in comparison to toughness of <0.5 J g^{-1} and elongation at break of <5% of polystyrene single fibers. The concentric triaxial morphology showed great advantage in comparison to the coaxial structure. Toughness and elongation at break were 1376 and 628% higher, respectively, for triaxial morphology in comparison to the coaxial fibers because of the better interface from the sandwich structure.

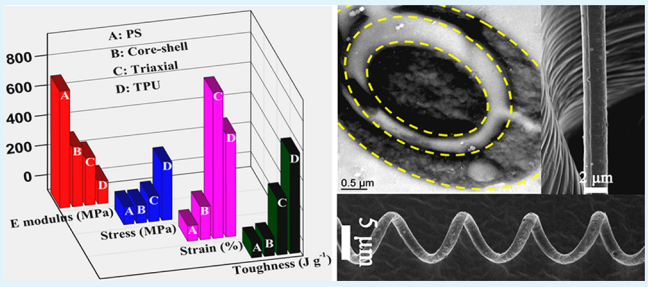

KEYWORDS: *electrospinning, triaxial fibers, mechanical properties, tough, 1D composites*

1. INTRODUCTION

Electrospinning is a simple processing method for the formation of ultra-fine fibers with diameters ranging from several micrometers to a few nanometers.[1−4] Because of the unique properties, such as the small diameter, large surface area/volume ratio, porosity, high aspect ratio, good mechanical properties,[5] and wide material choice for nanofibers, the electrospun nanofibers have been used for a broad range of applications, such as tissue engineering,[6] cell culture,[7] drug release,[8] air and liquid filtration,[9] battery separators,[10] and many others, including nanofiber-reinforced composites.[11−13]

The novel modifications on the conventional electrospinning nozzles provide opportunities to combine two or more components and incorporate more functions into one nano-/microfiber. Therein, coaxial electrospinning has attracted much attention for the efficient preparation of core−shell/hollow fibers. Various materials, including polymers, oligomers, metal salts, proteins, oils, and even cells/bacteria/viruses could be immobilized into the core of the core−shell fibers.[14−18] Bicomponent side-by-side electrospinning has been further developed to form nanofibers with novel properties by combining properties of each component. For example, Liu et al. reported a highly efficient bicomponent TiO_2/SnO_2 nanofiber photocatalyst fabricated by side-by-side electrospinning,[19] while Chen et al. studied the formation and mechanical properties of the nano-spring bicomponent nanofibers by this technique.[20]

Triaxial electrospinning is another novel recent modification on traditional electrospinning. Via this technique, three different polymer solutions could be electrospun into one nano-/microfiber with concentric three-layer morphology. However, because of the complex fiber morphology and difficulties of the characterization of the tricomponent structures, until now, only countable studies were focused on using triaxial electrospinning.[21−25] Kalra et al. used triaxial nozzles for making nanofibers with block copolymers of polystyrene (PS)−polyisoprene sandwiched between two silica layers to study the effect of confinement on the self-assembly behavior.[21] Chen et al. prepared nanowires in a microtube structure via triaxial electrospinning.[22] The use of triaxial electrospinning for making drug-releasing multi-shell capsules and nanofibers has been shown by Kim et al.[23] and Han et al.,[24] respectively. The possibility of making multilayer biodegradable nanofibers (gelatin as the outer and inner layers with polycaprolactone as the middle layer) using triaxial electrospinning is shown by Rabolt et al.[25]

PS is an interesting thermoplastic polymer produced in large amounts and used for many different applications, mainly in the form of films and foams. Electrospinning made possible the formation of PS fibers,[26,27] and recently, the use of these fiber membranes for selective separation of water and low viscous oil was shown.[28] PS fibers are brittle with very low strain at break (<2%) and toughness[29] that limit their use for many applications. A number of authors convincingly show a drastic increase in strain to break for different heterogeneous PS systems, such as multi-layered tapes based on PS−polyphenylene ether (PPE) layers alternating with polyethylene (PE), with a layer thickness of ca. 50 nm,[30] and PS filled with non-adhering core-shell rubbers of 200[31] or 100 nm.[32] Ding et al. electrospun polyamide 6 (PA6) or polyacrylonitrile (PAN)

Received: February 9, 2014
Accepted: March 31, 2014
Published: March 31, 2014

simultaneously with PS using a four-jet electrospinning process with four different syringes to reinforce PS fibrous mats.[33,34] An increase in tensile strength was observed depending upon the amount of PA6 or PAN fibers, but the strain at break was still very low (~30%). Thermoplastic polyurethane (TPU) fibers possess high ductility, high elongation, and high toughness,[35] and, therefore, are excellent candidates for reinforcing brittle polymers.

In the present work, we highlight the formation of tri-layered one-dimensional (1D) polymeric fibers (PS–TPU–PS), with TPU in the middle layer to reinforce and toughen brittle polymer fibers, such as PS. Electrospinning was used as a tool for generating this morphology in one step using a triaxial concentric nozzle. Tri-layer fibrous morphology was expected to provide a sandwich structure with a good interface between incompatible PS and TPU. Mechanical properties of single PS–TPU–PS triaxial fibers are reported in comparison to the corresponding single-component and core–shell TPU–PS fibers. High toughness (>270 J g^{-1}) with very high elongation at break (~700%) was achieved. This is in contrast to highly brittle PS fibers (toughness of <0.5 J g^{-1} and elongation at break of <5%). This is an interesting way of improving properties, even using incompatible polymers.

2. EXPERIMENTAL SECTION

2.1. Materials. PS (M_w = 230 000, and ρ = 1.02 g/cm^3), tetrahydrofuran (THF, ≥99.8%), and *N*,*N*′-dimethylformamide (DMF, ≥99.8%) were purchased from Sigma-Aldrich. TPU (Desmopan DP 2590A, ρ = 1.20 g/cm^3) was kindly supplied by Bayer Materials Science. All of the materials were used as received without further purification.

2.2. Characterizations. Tensile tests of single electrospun fibers were performed on a micro-tensile testing machine (JSF10, Power-each, Shanghai, China). The machine is equipped with a micro-load sensor (ULA-10GR, Minebea Co., Ltd., Japan), which has a load measuring range from 0.01 to 98.07 mN and a load resolution up to 0.0001 mN. The machine is driven by a stepper motor (BSHB366, Shenzhen Baishan Mechatronics Co., Ltd., China), which offers a high step resolution up to 0.1 μm. The testing speed was 0.094 mm/min. JSF10 software was used to control the machine and acquire data. The surface morphology and diameter of the single fibers were characterized by scanning electron microscopy (SEM, Zeiss LEO 1530, EHT = 2 kV). Prior to scanning, the samples were sputter-coated with platinum for 3.0 nm. Bright-field transmission electron microscopy (TEM) for looking at the cross-section samples of the triaxial fibers was performed on a Zeiss LEO 922 OMEGA electron microscope operated at 200 kV. The cross-section samples were prepared by embedding the aligned triaxial fiber belt into epoxy resin and stained with OsO_4 for better contrast. Differential scanning calorimetry (DSC) measurements were carried out on a Mettler Toledo DSC 821c using heating/cooling rates of 10 °C/min under a N_2 atmosphere. All of the samples were brought to the same thermal history by heating until 150 °C at a heating rate of 10 °C/min, followed by cooling to −100 °C at 10 °C/min. The phase transitions were evaluated using STARe software from the second heating cycle (from −100 °C to 225 °C at 10 °C/min). Attenuated total reflectance–infrared (ATR–IR) spectra were recorded on a Digilab Excalibur Series with an ATR unit MIRacle from Pike Technology.

2.3. Electrospinning. Triaxial electrospinning was carried out using a special concentric nozzle (inner diameters of 0.30, 1.20, and 2.20 mm, respectively) with PS solution inside and outside and TPU solution in the middle. PS was dissolved in DMF to form electrospinning solutions with concentrations of 0.3 g/mL. TPU solutions with a concentration of 0.18 g/mL was prepared by dissolving the TPU in DMF/THF = 4:1 (by weight). The applied voltage for the triaxial electrospinning was 20 kV. The flow rates of the inner PS, middle TPU, and outer PS solutions were 0.24, 0.60, and 0.60 mL/h, respectively. The single fibers were collected on a metal frame. The aligned triaxial nanofibers for cross-section observation by TEM were prepared by applying a voltage of 18 kV and collected in the form of a belt on a high-speed rotating disk with a rotating speed of 1500 rpm.

For comparison purposes, pure PS and pure TPU fibers were prepared by single nozzle electrospinning with applied voltages of 15 and 14.5 kV, flow rates of 0.24 and 0.6 mL/h, and spinning needles with inner diameters of 0.60 and 0.9 mm, respectively. The core–shell TPU–PS fibers were prepared by coaxial electrospinning with an applied voltage of 28 kV, a flow rate of 0.6 mL/h for TPU and 0.84 mL/h for PS, and a coaxial nozzle with an inner core diameter of 0.60 mm and an outer shell diameter of 1.10 mm. All of the fiber samples were collected with the same collecting distance of 25 cm.

2.4. Preparation and Tensile Tests of Single Electrospun Fiber Samples. The preparation of a single fiber for tensile tests was according to the previous report.[36] A stainless-steel frame with an inner rectangular size of 17.5 × 3.0 cm was used to collect the fibers. The fibers were picked by tweezers. A 0.2 mm thick paper frame with an inner rectangular size of 8 × 4 mm and two pieces of double-sided electrically conductive tape was used to catch the single fiber (Figure 1A). After that, two pieces of paper were used to cover the ends of the paper frame to make sure that the fiber was tightly adhered to the conductive tape (Figure 1A). During tests of single electrospun fibers, the paper frame with single electrospun fiber was mounted on the machine (Figure 1A). After cutting the right side of the paper frame, the single fiber was stretched by the single-fiber tensile test machine (panels B and C of Figure 1). The broken fiber segments on the paper frame (Figure 1D) after the tensile testing were used for SEM measurements to obtain the accurate diameter of the single fiber.

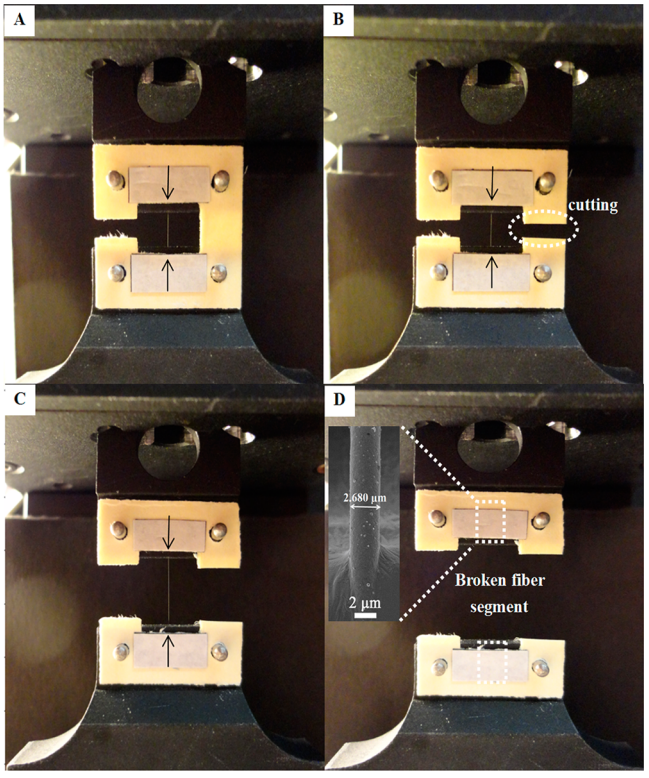

Figure 1. Digital photographs of electrospun single fiber for tensile test: (A) mounting the paper frame with single electrospun fiber (indicated by arrows) on the machine, (B) cutting the paper frame and (C) stretching the single electrospun fiber, and (D) collecting the broken fiber segments for SEM measurements.

A diameter displacement method was taken in this experiment based on the relationship between the tensile strength (σ), cross-section area (A) or diameter (D) of fiber, and applied load (F, detected

by the load sensor of the machine), as shown in the following equation:[36−38]

$$\sigma = \frac{F}{A} = \frac{F}{\frac{1}{4}\pi D^2} \quad (1)$$

During the testing, we assumed that all of the single fibers have a diameter of 1.000 μm (D_1) and the accurate fiber diameter (D_2) was measured using SEM. Therefore, the real tensile strength (σ_2) could be calculated by the following equations:

$$\sigma_1 = \frac{F}{\frac{1}{4}\pi {D_1}^2} \quad (2)$$

$$\sigma_2 = \frac{F}{\frac{1}{4}\pi {D_2}^2} \quad (3)$$

$$\sigma_2 = \sigma_1 \frac{{D_1}^2}{{D_2}^2} \quad (4)$$

where the tensile strength (σ_1) and tensile load (F) were directly obtained from the software of the tensile test machine, on the basis of the assumption of the fiber diameter (D_1 = 1.000 μm).

3. RESULTS AND DISCUSSION

3.1. Morphological Studies. The triaxial fibers presenting a concentric structure and layered morphology, as seen by TEM, are shown in the top of Figure 2. An aligned fiber belt collected on a rotating disk (rotation speed of 1500 rpm) was used for cross-section morphological studies by TEM. Although a clear triaxial structure was visible, the dimensions of the three layers could not be taken with accuracy because polyurethane swells in the embedding epoxy resin. The single triaxial fibers used for the determination of mechanical properties were collected on a stainless-steel frame, and SEM pictures were used for fiber thickness. The single fibers were smooth, with an average diameter of around 2.0 μm. For comparison purposes, the corresponding single-component fibers (PS and TPU) and bicomponent fibers (core−shell and TPU−PS) were also studied and showed uniform morphology (bottom of Figure 2). Because the fiber diameter below 250 nm diameter could affect the fiber mechanical properties in a drastic way (size-dependent effect)[38−40] and the failure mechanism, namely, transition from (multiple) crazing to complete shear yielding,[29] thick TPU−PS fibers of different morphologies (coaxial and triaxial) were made with a diameter of around 2.1 ± 0.4 μm to rule out the size-dependent effect.

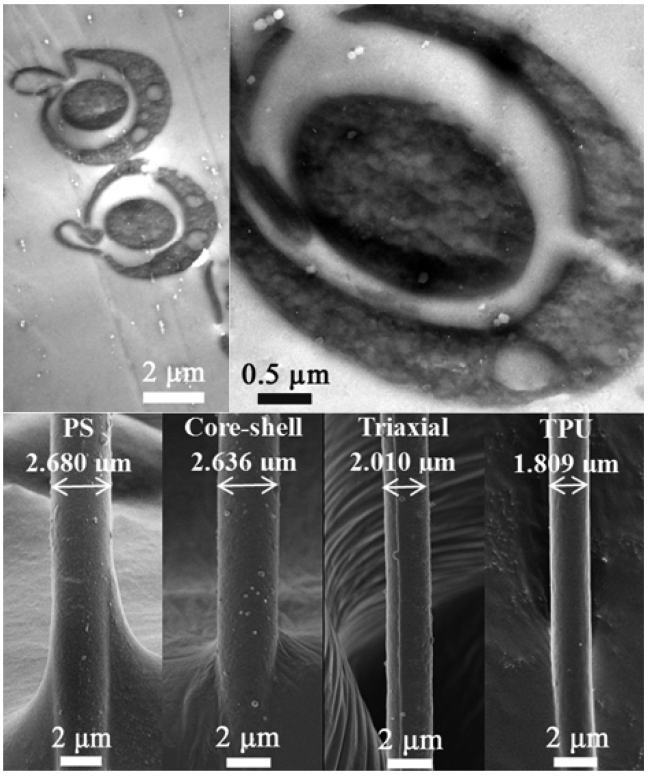

Figure 2. (Top) TEM of 1D composite fibers (PS−TPU−PS) with triaxial morphology and (bottom) SEM photos of the surface morphology and diameter of typical single fibers.

3.2. Mechanical Properties of Single Electrospun Fibers. PS single fibers were brittle with a very low strain (<4%) and stress at break (20 MPa) in comparison to highly elastic TPU single fibers (strain of ∼600% and stress of ∼300 MPa at break) (Figure 3 and Table 1). Combining TPU and PS

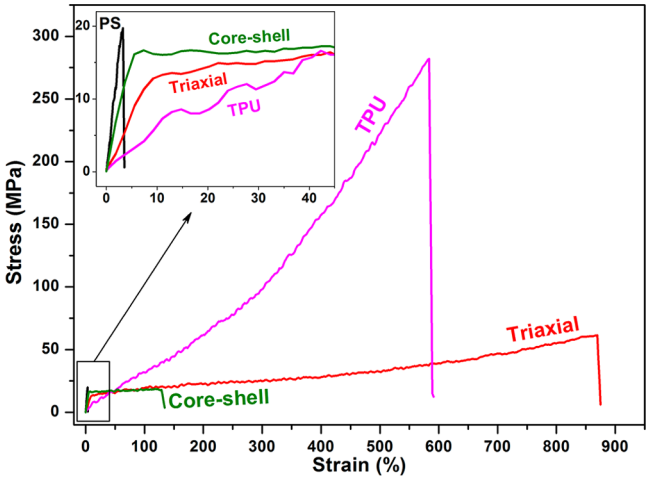

Figure 3. Typical stress−strain curves of single electrospun nanofibers in tensile load.

in a core−shell single-fiber morphology [70:30 (wt/wt) PS−TPU] led to an increase in strain at break (∼120 %) and increase in toughness from 0.4 J g^{-1} for monolithic PS fiber to 18.6 J g^{-1} for core−shell TPU−PS fiber without significantly changing stress at break. Further combining PS and TPU in a single fiber with a concentric triaxial morphology with 30 wt % TPU sandwiched between two layers of PS led to significant improvement in strain at break (∼873 %), stress at break (∼64 MPa), and toughness (∼274 J g^{-1}), as compared to single PS fibers and TPU−PS core−shell fibers.

Although TPU is a promising material for enhancement of mechanical properties, such as toughness and stretchability of brittle polymers, such as PS, the immiscibility of TPU and PS could lead to a poor interface, leading to a non-optimum increase in properties. TPU and PS made an immiscible blend as proven by the absence of any interaction from ATR−IR spectra and DSC results. Figure 4 presented the ATR−IR spectra of TPU, PS, core−shell, blend, and triaxial fibers. The core−shell and blend fibers had the same weight ratio of PS and TPU as triaxial fibers [70:30 (wt/wt) PS−TPU]. The characteristic peaks of both TPU and PS were seen in all samples, as marked in Figure 4. No shift of wave numbers was observed, indicating the absence of molecular interactions

Table 1. Summary of Mechanical Properties of Single Electrospun Nanofibers in Tensile Load

single fiber	*E* modulus (MPa)	stress (MPa)	strain at break (%)	toughness (J g^{-1})	diameter (μm)
PS	682.7 ± 44.3	19.8 ± 1.5	3.6 ± 0.5	0.4 ± 0.1	1.767 ± 0.121
core−shell	293.9 ± 105.6	18.8 ± 0.7	120.0 ± 12.9	18.6 ± 2.6	2.552 ± 0.137
triaxial	216.6 ± 32.1	63.7 ± 4.3	873.6 ± 25.5	274.5 ± 20.2	1.762 ± 0.065
TPU	48.3 ± 12.9	283.5 ± 13.5	588.9 ± 14.9	566.8 ± 38.1	1.485 ± 0.053

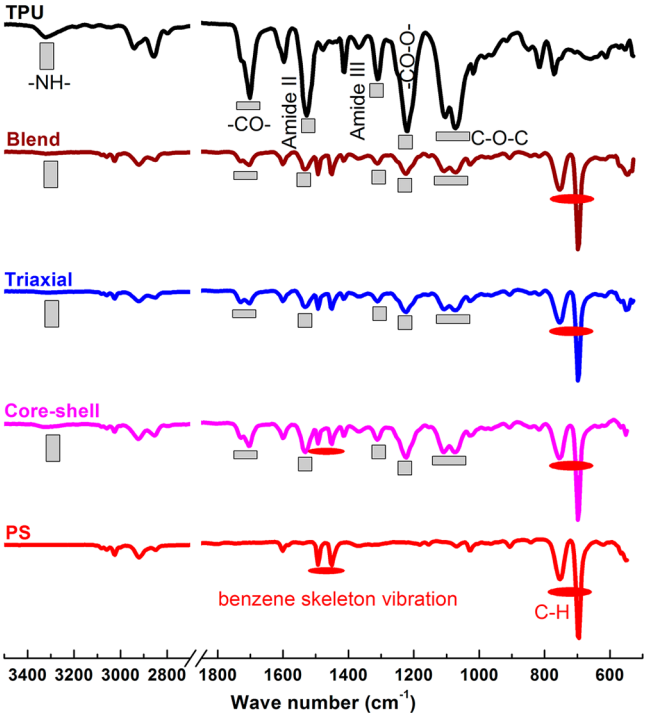

Figure 4. ATR−IR spectra of TPU, blend, triaxial, core−shell, and PS fibers.

between TPU and PS. Further studies on TPU fibers, blend fibers, and PS fibers by DSC also supported the conclusion of the immiscibility between TPU and PS. As shown in Figure 5, TPU and PS fibers presented glass transition temperatures at around −35 and 104 °C, respectively. There was no shift in the glass transition temperatures of TPU and PS in blend fibers, showing immiscibility of PS and TPU.

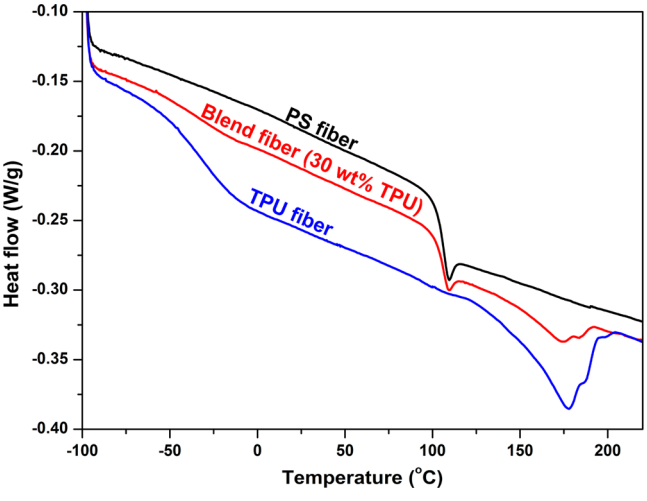

Figure 5. DSC curves of TPU, blend, and PS fibers.

However, in the suggested (triaxial) tri-layer fibrous morphology, the two immiscible polymers were forced in a multi-layered structure. Confining the TPU between two layers of PS apparently introduces a significant level of interlayer adhesion, forming a strong interface, guaranteeing the interfacial stress transfer and providing significant improvement in the ductility and toughness of the PS. Still, the mechanism of the toughening is unclear and has to do with the intrinsic parameters of the sample, such as molecular structure, morphology, and layer thickness. The "critical thickness"[31] of PS, 0.05 μm, which apparently guarantees the transition from (multiple) crazing to complete shear yielding was not obtained in the studied samples.

3.3. Morphology of Single Electrospun Fiber during and after Tensile Tests. The fiber morphology was monitored during the tensile testing experiment by stopping the test before the sample broke, i.e., at different elongations (Figure 6). The concentric triaxial fibers maintained the

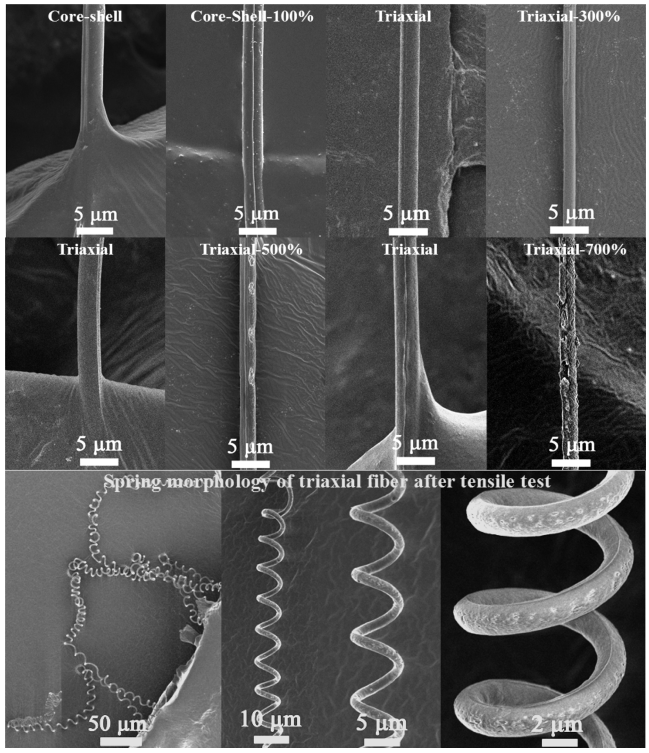

Figure 6. Morphologies of the single electrospun fibers during the tensile tests with different elongations and spring morphology of triaxial fiber after tensile test.

morphology until about 300% elongation without signs of cracks in the outer layer. At 500% elongation, some cracks were evident on the outer layer, which became more at 700% elongation, followed by failure of the fiber at 873%. The broken fibers showed spring morphology (Figure 4) because of

dx.doi.org/10.1021/am500837s | ACS Appl. Mater. Interfaces 2014, 6, 5918−5923

differential elongations of PS and TPU, as observed previously for nylon-6-reinforced TPU composites.[41]

4. CONCLUSION

A combination of appropriate reinforcing material and morphology is necessary for the properties improvement of a polymeric fibrous material. Significant improvement in the mechanical properties of PS fibers could be achieved by elastomeric TPU in combination with a three-layered triaxial fibrous morphology, with TPU being sandwiched by two layers of PS. The composite fibers were highly tough (toughness of >270 J g^{-1}) and could be elongated without any signs of cracks until about 300% in comparison to highly brittle PS fibers (toughness of <0.5 J g^{-1} and elongation at break of <5%). Moreover, triaxial morphology provided great advantage over coaxial morphology by showing a huge difference in mechanical properties. Toughness and elongation at break were 1376 and 628% higher, respectively, for triaxial morphology in comparison to the coaxial fibers because of the sandwich structure.

AUTHOR INFORMATION

Corresponding Author

*Telephone: +49-921-553397. Fax: +49-921-553393. E-mail: agarwal@uni-bayreuth.de.

Notes

The authors declare no competing financial interest.

ACKNOWLEDGMENTS

Authors would like to thank Deutsche Forschungsgemeinschaft (DFG) for financial support.

REFERENCES

(1) Li, D.; Xia, Y. Electrospinning of nanofibers: Reinventing the wheel? *Adv. Mater.* **2004**, *16*, 1151−1170.
(2) Greiner, A.; Wendorff, J. H. Electrospinning: A fascinating method for the preparation of ultrathin fibers. *Angew. Chem., Int. Ed.* **2007**, *46*, 5670−5703.
(3) Agarwal, S.; Greiner, A.; Wendorff, J. H. Functional materials by electrospinning of polymers. *Prog. Polym. Sci.* **2013**, *38*, 963−991.
(4) Wu, J.; Wang, N.; Zhao, Y.; Jiang, L. Electrospinning of multilevel structured functional micro-/nanofibers and their applications. *J. Mater. Chem. A* **2013**, *1*, 7290−7305.
(5) Arinstein, A.; Zussman, E. Electrospun polymer nanofibers: Mechanical and thermodynamic perspectives. *J. Polym. Sci., Part B: Polym. Phys.* **2011**, *49*, 691−707.
(6) Yoshimoto, H.; Shin, Y.; Terai, H.; Vacanti, J. A biodegradable nanofiber scaffold by electrospinning and its potential for bone tissue engineering. *Biomaterials* **2003**, *24*, 2077−2082.
(7) Sun, T.; Norton, D.; McKean, R. J.; Haycock, J. W.; Ryan, A. J.; MacNeil, S. Development of a 3D cell culture system for investigating cell interactions with electrospun fibers. *Biotechnol. Bioeng.* **2007**, *97*, 1318−1328.
(8) Zeng, J.; Xu, X.; Chen, X.; Liang, Q.; Bian, X.; Yang, L.; Jing, X. Biodegradable electrospun fibers for drug delivery. *J. Controlled Release* **2003**, *92*, 227−231.
(9) Yun, K. M.; Hogan, C. J., Jr.; Matsubayashi, Y.; Kawabe, M.; Iskandar, F.; Okuyama, K. Nanoparticle filtration by electrospun polymer fibers. *Chem. Eng. Sci.* **2007**, *62*, 4751−4759.
(10) Alcoutlabi, M.; Lee, H.; Watson, J. V.; Zhang, X. Preparation and properties of nanofiber-coated composite membranes as battery separators via electrospinning. *J. Mater. Sci.* **2013**, *48*, 2690−2700.
(11) Akangah, P.; Lingaiah, S.; Shivakumar, K. Effect of nylon-66 nano-fiber interleaving on impact damage resistance of epoxy/carbon fiber composite laminates. *Compos. Struct.* **2010**, *92*, 1432−1439.
(12) Jiang, S.; Hou, H.; Greiner, A.; Agarwal, S. Tough and transparent nylon-6 electrospun nanofiber reinforced melamine−formaldehyde composites. *ACS Appl. Mater. Interfaces* **2012**, *4*, 2597−2603.
(13) Jiang, S.; Duan, G.; Hou, H.; Greiner, A.; Agarwal, S. Novel layer-by-layer procedure for making nylon-6 nanofiber reinforced high strength, tough, and transparent thermoplastic polyurethane composites. *ACS Appl. Mater. Interfaces* **2012**, *4*, 4366−4372.
(14) Amler, E.; Mickova, A.; Buzgo, M. Electrospun core/shell nanofibers: A promising system for cartilage and tissue engineering? *Nanomedicine* **2013**, *8*, 509−512.
(15) Ji, W.; Sun, Y.; Yang, F.; Beucken, J. J. P.; Fan, M.; Chen, Z.; Jansen, J. Bioactive electrospun scaffolds delivering growth factors and genes for tissue engineering applications. *Pharm. Res.* **2011**, *28*, 1259−1272.
(16) Lee, G.; Song, J.-C.; Yoon, K.-B. Controlled wall thickness and porosity of polymeric hollow nanofibers by coaxial electrospinning. *Macromol. Res.* **2010**, *18*, 571−576.
(17) Agarwal, S.; Greiner, A.; Wendorff, J. H. Electrospinning of manmade and biopolymer nanofibers—Progress in techniques, materials, and applications. *Adv. Funct. Mater.* **2009**, *19*, 2863−2879.
(18) Korehei, R.; Kadla, J. F. Encapsulation of T4 bacteriophage in electrospun poly(ethylene oxide)/cellulose diacetate fibers. *Carbohydr. Polym.* **2014**, *100*, 150−157.
(19) Liu, Z.; Sun, D. D.; Guo, P.; Leckie, J. O. An efficient bicomponent TiO_2/SnO_2 nanofiber photocatalyst fabricated by electrospinning with a side-by-side dual spinneret method. *Nano Lett.* **2006**, *7*, 1081−1085.
(20) Chen, S.; Hou, H.; Hu, P.; Wendorff, J. H.; Greiner, A.; Agarwal, S. Effect of different bicomponent electrospinning techniques on the formation of polymeric nanosprings. *Macromol. Mater. Eng.* **2009**, *294*, 781−786.
(21) Kalra, V.; Lee, J. H.; Park, J. H.; Marquez, M.; Joo, Y. L. Confined assembly of asymmetric block-copolymer nanofibers via multiaxial jet electrospinning. *Small* **2009**, *5*, 2323−2332.
(22) Chen, H.; Wang, N.; Di, J.; Zhao, Y.; Song, Y.; Jiang, L. Nanowire-in-microtube structured core/shell fibers via multifluidic coaxial electrospinning. *Langmuir* **2010**, *26*, 11291−11296.
(23) Kim, W.; Kim, S. S. Synthesis of biodegradable triple-layered capsules using a triaxial electrospray method. *Polymer* **2011**, *52*, 3325−3336.
(24) Han, D.; Steckl, A. J. Triaxial electrospun nanofiber membranes for controlled dual release of functional molecules. *ACS Appl. Mater. Interfaces* **2013**, *5*, 8241−8245.
(25) Liu, W.; Ni, C.; Chase, D. B.; Rabolt, J. F. Preparation of multilayer biodegradable nanofibers by triaxial electrospinning. *ACS Macro Lett.* **2013**, *2*, 466−468.
(26) Casper, C. L.; Stephens, J. S.; Tassi, N. G.; Chase, D. B.; Rabolt, J. F. Controlling surface morphology of electrospun polystyrene fibers: Effect of humidity and molecular weight in the electrospinning process. *Macromolecules* **2003**, *37*, 573−578.
(27) Nitanan, T.; Opanasopit, P.; Akkaramongkolporn, P.; Rojanarata, T.; Ngawhirunpat, T.; Supaphol, P. Effects of processing parameters on morphology of electrospun polystyrene nanofibers. *Korean J. Chem. Eng.* **2012**, *29*, 173−181.
(28) Lee, M. W.; An, S.; Latthe, S. S.; Lee, C.; Hong, S.; Yoon, S. S. Electrospun polystyrene nanofiber membrane with superhydrophobicity and superoleophilicity for selective separation of water and low viscous oil. *ACS Appl. Mater. Interfaces* **2013**, *5*, 10597−10604.
(29) Smit, R. J. M.; Brekelmans, W. A. M.; Meijer, H. E. H. Predictive modelling of the properties and toughness of polymeric materials. Part I: Why is polystyrene brittle and polycarbonate tough? *J. Mater. Sci.* **2000**, *35*, 2855−2867.
(30) Van der Sanden, M. C. M.; Buijs, L. G. C.; De Bie, F. O.; Meijer, H. E. H. Deformation and toughness of polymeric systems: 5. A critical examination of multilayered structure. *Polymer* **1994**, *35*, 2783−2792.
(31) Van der Sanden, M. C. M.; Meijer, H. E. H.; Lemstra, P. J. Deformation and toughness of polymeric systems: 1. The concept of a critical thickness. *Polymer* **1993**, *34*, 2148−2154.

(32) Jansen, B. J. P.; Meijer, H. E. H.; Lemstra, P. J. Processing of (in)tractable polymers using reactive solvents: Part 5: Morphology control during phase separation. *Polymer* **1999**, *40*, 2917−2927.
(33) Li, X.; Ding, B.; Lin, J.; Yu, J.; Sun, G. Enhanced mechanical properties of superhydrophobic microfibrous polystyrene mats via polyamide 6 nanofibers. *J. Phys. Chem. C* **2009**, *113*, 20452−20457.
(34) Sun, M.; Li, X.; Ding, B.; Yu, J.; Sun, G. Mechanical and wettable behavior of polyacrylonitrile reinforced fibrous polystyrene mats. *J. Colloid Interface Sci.* **2010**, *347*, 147−152.
(35) Alhazov, D.; Gradys, A.; Sajkiewicz, P.; Arinstein, A.; Zussman, E. Thermo-mechanical behavior of electrospun thermoplastic polyurethane nanofibers. *Eur. Polym. J.* **2013**, *49*, 3851−3856.
(36) Chen, F.; Pen, X.; Li, T.; Chen, S.; Wu, X.-F.; Reneker, D. H.; Hou, H. Mechanical characterization of single high-strength electrospun polyimide nanofibres. *J. Phys. D: Appl. Phys.* **2008**, *41*, 025308.
(37) Vasiliev, V. V.; Morozov, E. V. *Mechanics and Analysis of Composite Materials*; Elsevier Science, Ltd.: Amsterdam, Netherlands, 2001.
(38) Papkov, D.; Zou, Y.; Andalib, M. N.; Goponenko, A.; Cheng, S. Z. D.; Dzenis, Y. A. Simultaneously strong and tough ultrafine continuous nanofibers. *ACS Nano* **2013**, *7*, 3324−3331.
(39) Arinstein, A.; Burman, M.; Gendelman, O.; Zussman, E. Effect of supramolecular structure on polymer nanofibre. *Nat. Nanotechnol.* **2007**, *2*, 59−62.
(40) Wang, W.; Barber, A. H. Diameter-dependent melting behaviour in electrospun polymer fibres. *Nanotechnology* **2010**, *21*, 225701.
(41) Jiang, S.; Greiner, A.; Agarwal, S. Short nylon-6 nanofiber reinforced transparent and high modulus thermoplastic polymeric composites. *Compos. Sci. Technol.* **2013**, *87*, 164−169.